Geophys. J. Int. (2004) **157,** 341–353 doi: 10.1111/j.1365-246X.2004.02175.x

Shear wave anisotropy beneath the Cascadia subduction zone and western North American craton

Claire A. Currie,[1,2,*] John F. Cassidy,[2,1] Roy D. Hyndman[2,1] and Michael G. Bostock[3]

[1]*School of Earth and Ocean Sciences, University of Victoria, Victoria, BC, Canada*
[2]*Pacific Geoscience Centre, Geological Survey of Canada, Sidney, BC, Canada*
[3]*Department of Earth and Ocean Sciences, University of British Columbia, Vancouver, BC, Canada*

Accepted 2003 October 10. Received 2003 October 1; in original form 2003 February 28

SUMMARY

We have examined shear wave splitting of *SKS* phases at 26 permanent broadband stations in western North America to constrain regional trends in anisotropy at the Cascadia subduction zone (CSZ) and adjacent regions. At forearc stations above the Juan de Fuca Plate, the fast directions are approximately parallel to the direction of absolute plate motion of the main Juan de Fuca Plate (∼N70°E). Delay times of 1.0 to 1.5 s indicate a mantle source for the anisotropy, most likely strain-induced lattice-preferred orientation of anisotropic mantle minerals. The anisotropy may be related to present-day subduction-induced deformation of the mantle beneath the subducting plate. The delay times show an increase with distance from the deformation front (trench), which may be indicative of 3–5 per cent anisotropy within the forearc mantle wedge, with a fast direction parallel to the subduction direction. Above the Explorer Plate at the northern end of the CSZ, the fast directions are N25°E. This may reflect either the more northerly subduction direction of that plate, or a transition from subduction-related deformation to along-margin flow parallel to the transcurrent Queen Charlotte Fault to the north. At four stations in the central backarc of the CSZ, fast directions are parallel to the Juan de Fuca–North America convergence direction, consistent with mantle deformation due to subduction-induced mantle wedge flow, as well as deformation of the uppermost backarc mantle associated with motion of the overriding plate. No clear splitting was observed at the two most northern backarc stations, indicating either little horizontal anisotropy or highly complex anisotropy beneath these stations, possibly associated with complex mantle flow around the northern edge of the subducted plate. The hot, thin backarc lithosphere of the Cascadia subduction zone extends to the Rocky Mountain Trench, the western boundary of the cold, stable North America craton. At two stations on the North America craton the shear wave splitting parameters show significant azimuthal variations with a 90° periodicity, characteristic of multiple layers of anisotropy. The observations were fitted with a two-layer model with an upper anisotropic layer with a fast direction of N12°E and delay time of 1.4 s, and a lower layer with a fast direction of N81°E and delay time of 2.0 s. The North America craton is characterized by a thick lithosphere. Thus, the two anisotropic layers may reflect an upper layer of fossil anisotropy within the cool (<900 °C) lithosphere and an underlying anisotropic layer produced by present-day deformation.

Key words: anisotropy, Cascadia subduction zone, mantle deformation, mantle flow, shear wave splitting, *SKS*.

1 INTRODUCTION

Seismic anisotropy within the mantle has been documented in a number of tectonic settings worldwide, including subduction zones, spreading centres and stable cratons. Mantle anisotropy is generally attributed to shear deformation, where simple shear results in a lattice-preferred orientation (LPO) of anisotropic mantle minerals, primarily olivine (e.g. Nicolas & Christensen 1987; Silver & Chan 1991). Laboratory studies show that under moderate to large strains, the *a*-axis of olivine will become aligned in the direction of maximum finite extension (Karato 1987; Nicolas & Christensen 1987) or in the direction of mantle flow (Zhang & Karato 1995). This alignment is only produced when dislocation creep is the dominant deformation mechanism (Karato 1987; Nicolas & Christensen 1987; Karato 1989).

*Corresponding author: Pacific Geoscience Centre, Geological Survey of Canada, PO Box 6000, 9860 West Saanich Road, Sidney, BC, V8L 4B2, Canada. E-mail: ccurrie@nrcan.gc.ca

One of the key factors controlling the development of LPO is temperature (Savage 1999 and references therein). At temperatures greater than 900 °C, mantle minerals will develop LPO under moderate shear strain, and thus anisotropy can be actively produced by present-day mantle deformation. If the temperature is then decreased to less than 900 °C, anisotropy may become 'frozen in', leading to fossil anisotropy. Present-day mantle deformation has been invoked to explain anisotropy in tectonically active regions, such as subduction zones and spreading centres (e.g. Vinnik *et al.* 1992). On the other hand, anisotropy over stable cratons has been explained by fossil anisotropy within the lithosphere produced by the most recent tectonic event (Silver & Chan 1991), sublithospheric mantle flow (Fouch *et al.* 2000), or a combination of both (Vinnik *et al.* 1992; Levin *et al.* 1999; Fouch *et al.* 2000).

Seismic anisotropy can be observed through shear wave splitting of *SKS* waveforms. When a shear wave passes through an anisotropic medium, it splits into two orthogonal components which travel at different velocities. Shear wave splitting is characterized by two parameters: the polarization direction of the first arriving shear wave at the Earth's surface (the fast direction), and the delay time between the two shear waves. Because *SKS* waves are teleseismic shear waves that are generated by conversion of *P* waves at the core–mantle boundary, any observed anisotropy is confined to the travel path from that boundary to the receiver. The fast direction of shear wave splitting is generally assumed to be parallel to the horizontal projection of the olivine a-axis. Thus, observations of seismic anisotropy can be used to constrain the orientation of the local strain field within the mantle. The delay time depends on the thickness of the anisotropic layer and the magnitude of the anisotropy within the layer.

In the current study, we have used *SKS* splitting observations to constrain mantle anisotropy beneath the northern Cascadia subduction zone and adjacent regions (Fig. 1). In the study area, the Juan de Fuca and Explorer plates subduct beneath the North America plate. Both are young oceanic plates, with ages less than 8 Myr (Riddihough 1984). The Juan de Fuca Plate subducts at a rate of 4.0–4.5 cm yr^{-1} (Riddihough 1984; Gripp & Gordon 2002). Riddihough (1984) suggests that the Explorer Plate broke from the main Juan de Fuca Plate and began moving as an independent plate at 4 Ma. Recent GPS observations indicate that there is approximately 2 cm yr^{-1} convergence between the North America and Explorer plates at the southern end of the Explorer–North America margin, with convergence rates decreasing to the north (Mazzotti *et al.* 2002). Models of relative plate motion constrained by seafloor magnetic anomalies, GPS observations and earthquake focal mechanisms suggest that Explorer Plate convergence is more northerly than Juan de Fuca Plate convergence (Riddihough 1977; Mazzotti *et al.* 2002; Ristau *et al.* 2002). The Explorer Plate may also be in the process of breaking up (Rohr & Furlong 1995; Braunmiller & Nabelek 2002). The northern limit of the present subduction zone is the triple junction between the Pacific, North America and Explorer plates. Over the last 4 Myr, the triple junction has migrated north from offshore central Vancouver Island to its present position west of the northern tip of Vancouver Island (Riddihough 1977). North of the triple junction, the margin changes from subduction to dextral strike-slip motion along the Queen Charlotte Fault system.

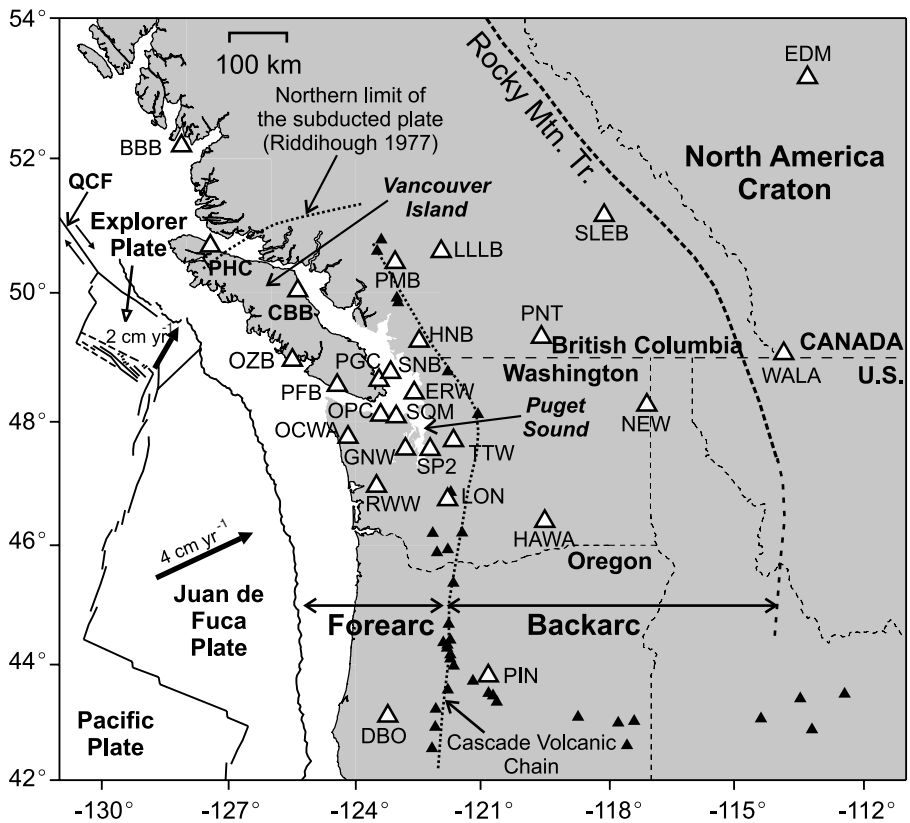

Figure 1. Map of the Cascadia subduction zone showing the distribution of seismograph stations used in this study (open triangles). Solid triangles are active volcanoes. QCF is the Queen Charlotte Fault. The Rocky Mountain Trench (dashed line) is taken to define the landward extent of the Cascadia backarc, eastward of which lies the North America craton.

The forearc region of the Cascadia subduction zone is limited on its eastern edge by the active Cascade Volcanic Chain. We take the backarc to be the high-temperature, thin lithosphere region that extends eastward from the Cascade Volcanic Chain. The eastern limit of this region is concluded to coincide with the Rocky Mountain Trench (RMT). There is a pronounced change in lithospheric properties from the west side to the east side of the RMT, including an increase in continental crust thickness from ∼35 to ∼50 km, an increase in *Pn* velocities from ∼7.8 km s^{-1} to ∼8.1 km s^{-1}, and a decrease in surface heat flow from 80–100 mW m^{-2} to ∼45 mW m^{-2} (Hyndman & Lewis 1999 and references therein). This boundary correlates well with the edge of a high-velocity region observed in seismic tomography studies to depths greater than 250 km (e.g. Grand 1994; Fredericksen *et al.* 2001). These observations have been interpreted as the juxtaposition of the thin (55–60 km), warm backarc lithosphere against the thick (>250 km), cool lithosphere of the North America craton (Hyndman & Lewis 1999).

This region offers an opportunity to examine patterns of seismic anisotropy within an active convergent margin, as well as across the transition to a stable craton. From these observations, patterns of mantle strain can be inferred and constraints can be placed on mantle dynamics.

2 DATA ANALYSIS

We have examined data from 26 seismic stations across the study region (Fig. 1). The Canadian stations are part of the Canadian National Seismic Network, maintained by the Geological Survey of Canada. The stations in Washington and Oregon are part of the Pacific Northwest Seismic Network, maintained by the University of Washington and the US Geological Survey. All sites are permanent stations with three-component broadband instruments, sampled at rates between 40 and 100 Hz. Periods of continuous operation range from 2 yr to more than 10 yr. This station distribution covers both the forearc and backarc regions of the northern Cascadia subduction zone, allowing us to examine trends in anisotropy along the strike of the margin as well as perpendicular to the margin. We have examined data at station BBB, ∼250 km northeast of the triple junction that marks the northern limit of the subduction zone, to look at variations in anisotropy associated with the transition from subduction to transcurrent motion. We have also analysed data at stations EDM and WALA, near the western edge of the North America craton, to compare the anisotropy within this region with that of the subduction system.

At each station, we analysed shear wave splitting of *SKS* phases from earthquakes at distances of 85° to 140° from each station. At these distances, the incidence angle of the *SKS* energy at the station is within 15° of vertical. The near-vertical incidence angle leads to a high lateral resolution (∼50 km) for the subsurface anisotropic structure, and complications from near-surface reverberations and phase conversions are minimized (Nuttli 1961; Crampin 1977). At each station, data were chosen for analysis based on a high signal-to-noise ratio, a small amplitude of the *SKS* phase on the vertical component and a large time gap (>15 s) before the next significant phase arrival.

The final data set contains earthquakes from a wide range of azimuths. At most stations, the only backazimuth with no data is from N10°E to N125°E. The number of earthquakes at some stations is small, as these stations have operated for less than 2 yr. A low-pass Butterworth filter with a corner frequency of 0.15 Hz was applied to each waveform to remove high-frequency noise that complicated the *SKS* arrival. The *SKS* energy has a dominant frequency between 0.05 and 0.15 Hz, and thus the effects of the filter on the *SKS* waveform are small. For a small number of earthquakes, the unfiltered data could be used for the splitting analysis. A comparison of the shear wave splitting parameters for the filtered and unfiltered data showed that they are similar. We report only the results for the filtered data.

For each waveform, the Silver & Chan (1991) method was used to find the shear wave splitting parameters and their uncertainties. This approach uses a grid search over all possible fast directions and delay times between 0 and 3 s for the pair of splitting parameters that minimizes the energy on the transverse component, after each pair has been applied to the data to remove the splitting (i.e. the data are corrected for splitting). An example of the original data and the corrected data is given in Fig. 2. The grid search yields a contour plot of the energy on the corrected transverse component for each fast direction–delay time pair, allowing the uncertainties of each splitting parameter to be quantified. A well-constrained result will have a contour plot with a well-defined ellipsoidal minimum (e.g. Fig. 2c). In some cases, the minimum is highly elongated along the delay time axis. This signifies the absence of detectable splitting (a null result). A null result can be due to: (1) the absence of significant horizontal anisotropy, (2) complex anisotropy, such as

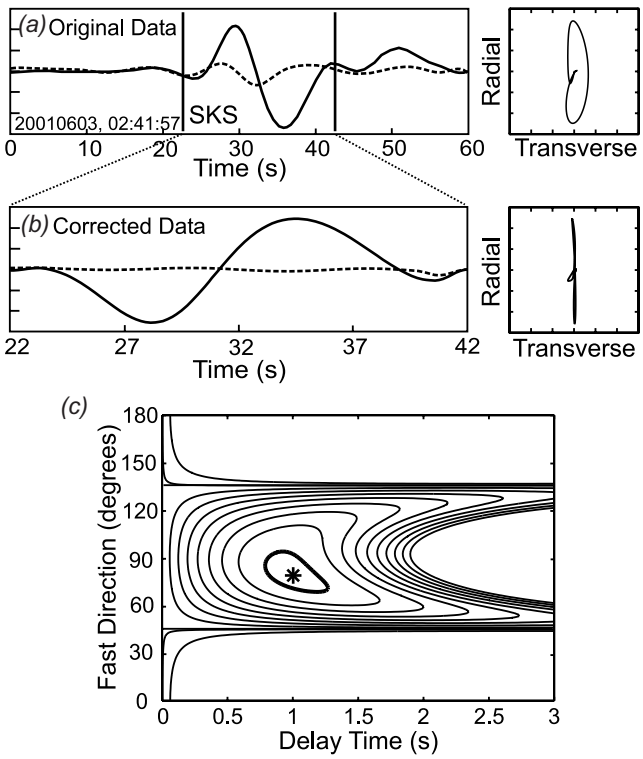

Figure 2. An example of data recorded at station PGC. The magnitude 7.2 earthquake occurred on 2001 June 3 in the Kermadec Islands region (29.7°S, 178.6°W) at a depth of 178 km. The backazimuth and incidence angle of the energy are 226° and 9.8°, respectively. (a) The original, filtered radial (solid) and transverse (dashed) horizontal components. The vertical lines indicate the *SKS* window used for analysis. The particle motion plot for the *SKS* window is shown on the right. (b) Radial and transverse components, corrected for splitting. Almost all the *SKS* energy has been removed from the transverse component. The particle motion plot (right) shows a linear particle motion. (c) Contour plot of the energy on the corrected transverse component, showing the minimum value (fast direction N80°E, delay time 1.0 s) with the 95 per cent confidence interval (thick line) and multiples of that contour interval.

multiple or steeply dipping anisotropic layers, or (3) a fast direction that is parallel or perpendicular to the polarization direction of the incoming energy for a single horizontally anisotropic layer. For the *SKS* arrivals, the initial polarization direction should be equal to the backazimuth.

For quality control on each observation, splitting analysis was also performed using the particle motion linearization method (Silver & Chan 1991). This alternative method searches for the pair of splitting parameters that results in the most linear particle motion for the corrected waveforms. For the data included in this study, good agreement was observed between the two methods, with typical differences in fast directions of less than 10° and delay time differences of less than 0.3 s. Each splitting result was rated as excellent, good or fair, based on the quality of the data (high signal-to-noise ratio, a clear *SKS* waveform), the quality of the energy minimization contour plot and the agreement between the two analysis methods.

3 SHEAR WAVE SPLITTING OBSERVATIONS

Only three stations (BBB, LLLB, SLEB) did not have resolvable splitting for data from a wide range of azimuths (Table 1). We have classified these stations as null stations. The numerous null results suggest that there is either only weak horizontal anisotropy or highly complex anisotropy beneath these stations.

At all other stations, significant shear wave splitting was observed (Table 1). Fig. 3 shows lower-hemisphere projections of the fast directions and delay times at 10 stations. Most waveforms that yielded null results lie at backazimuths that are nearly parallel or perpendicular to the fast directions obtained for most other earthquakes at that station. This indicates that the absence of splitting on these waveforms is due to the polarization direction being parallel or perpendicular to the fast direction of anisotropy.

Table 1. Number of splitting and null observations at each station, with the stacked shear wave splitting parameters (fast direction (ϕ) and delay time (dt), with 95 per cent confidence intervals).

Station	Lat. (°N)	Long. (°E)	#split	#null	ϕ	$\pm\phi$	dt (s)	$\pm$dt (s)
BBB[1]	52.18	−128.11	1	15	–	–	–	–
CBB	50.03	−125.37	7	5	22	13.5	1.23	0.38
EDM[2]	53.22	−113.35	14	3	–	–	–	–
HNB	49.27	−122.58	6	2	66	11.5	1.25	0.44
LLLB[1]	50.61	−121.88	1	16	–	–	–	–
OZB	48.96	−125.49	5	2	60	29	0.50	0.31
PFB	48.57	−124.44	2	3	75	15	0.77	0.39
PGC	48.65	−123.45	12	10	77	19	1.03	0.39
PHC	50.71	−127.43	10	6	30	22	0.88	0.44
PMB[3]	50.51	−123.06	3	–	45	–	0.65	–
PNT	49.31	−119.61	18	5	58	4.5	1.33	0.40
SLEB[1]	51.17	−118.13	4	14	–	–	–	–
SNB	48.78	−123.17	8	9	86	14.5	1.13	0.51
WALA[2]	49.05	−113.91	18	9	–	–	–	–
DBO	43.12	−123.24	2	1	54	15	1.7	0.5
ERW	48.45	−122.63	2	2	79	13	1.41	0.26
GNW	47.56	−122.83	8	2	69	11	1.08	0.35
HAWA	46.39	−119.53	1	1	74	6.5	1.08	0.3
LON	46.75	−121.81	5	4	93	21.5	0.82	0.38
NEW	48.26	−117.12	6	2	71	7	1.48	0.46
OCWA	47.75	−124.18	1	0	57	10.5	1.75	0.78
OPC	48.10	−123.41	3	0	55	19	0.92	0.41
PIN	43.81	−120.87	1	0	64	1.5	2.08	0.1
RWW	46.96	−123.54	3	1	68	9	0.78	0.32
SP2	47.56	−122.25	5	2	65	7.5	0.89	0.45
SQM	48.08	−123.05	2	1	57	10.5	2.16	1.06
TTW	47.69	−121.69	6	2	65	9.5	1.54	0.54

[1]Null results for most waveforms.
[2]Significant azimuthal variations in splitting parameters.
[3]Measurements from Bostock & Cassidy (1995).

Azimuthal variations in the splitting parameters are indicative of complex anisotropy beneath the station, such as small-scale lateral variations in anisotropy, dipping anisotropic layers or multiple anisotropic layers. The only stations for which a clear azimuthal variation in the splitting parameters can be identified are stations EDM and WALA, located on the North America craton (Fig. 3 and Section 4.4). At all other stations with a good azimuthal distribution of high-quality data there are no significant azimuthal variations in the splitting parameters (e.g. stations PGC, SNB, PNT on Fig. 3). For nearby stations with a poorer azimuthal coverage, we assumed that there is also little variation.

In order to obtain a single set of splitting parameters at each station except EDM and WALA, the splitting results were stacked using the approach of Wolfe & Silver (1998). At each station, the transverse energy contour plots for each waveform were normalized by their minimum value. The normalized contour plots were then summed, yielding a contour plot with the average fast direction and delay time for that station, along with their 95 per cent confidence limits. By using normalized contour plots, the waveforms with the most well-constrained parameters were weighted more heavily in the summation. We included all non-null results in the stacking procedure. The inclusion of null results yields a similar average fast direction and delay time for that station, but with larger uncertainties. Fig. 4 shows the fast directions and delay times obtained from stacking the data (see also Table 1). The stacked results at each station were classified as either well-constrained or poorly constrained. For a well-constrained stacked result, there had to be at least five good-quality waveforms with well-constrained splitting parameters from at least three distinct backazimuths. Below, we summarize the observations for each region.

3.1 Forearc observations

Most stations in this study are located within the forearc above the Juan de Fuca Plate (Fig. 4). At station DBO in Oregon, three waveforms were analysed. An average (stacked) fast direction of N54°E ± 15° with a delay time of 1.7 ± 0.5 s was obtained for two of the waveforms. The third earthquake waveform yielded a null result. This earthquake was at a backazimuth of N226°E, consistent with a NE–SW fast direction for this station.

At the forearc stations in Washington and southwest British Columbia, the stacked shear wave splitting parameters are very consistent between stations. Fast directions are approximately N70°E (Table 1). Delay times at the majority of stations are between 0.7 and 1.5 s. Two stations (OCWA and SQM) have delay times greater than 1.7 s, but these results are not well constrained due to the small number of earthquakes analysed and noisy data. These results are similar to previous *SKS* splitting observations by Bostock & Cassidy (1995) for station PGC and by Silver & Chan (1991) for station LON.

Inland of the Explorer Plate, the forearc stations CBB and PHC have fast directions of N22°E ± 14° and N30°E ± 22°, with delay times of 1.2 ± 0.4 s and 0.9 ± 0.4 s respectively. These fast directions are rotated ∼45° from those observed above the Juan de Fuca Plate. At station BBB, northeast of the Pacific–Explorer–North America triple junction, no clear anisotropy could be identified for 15

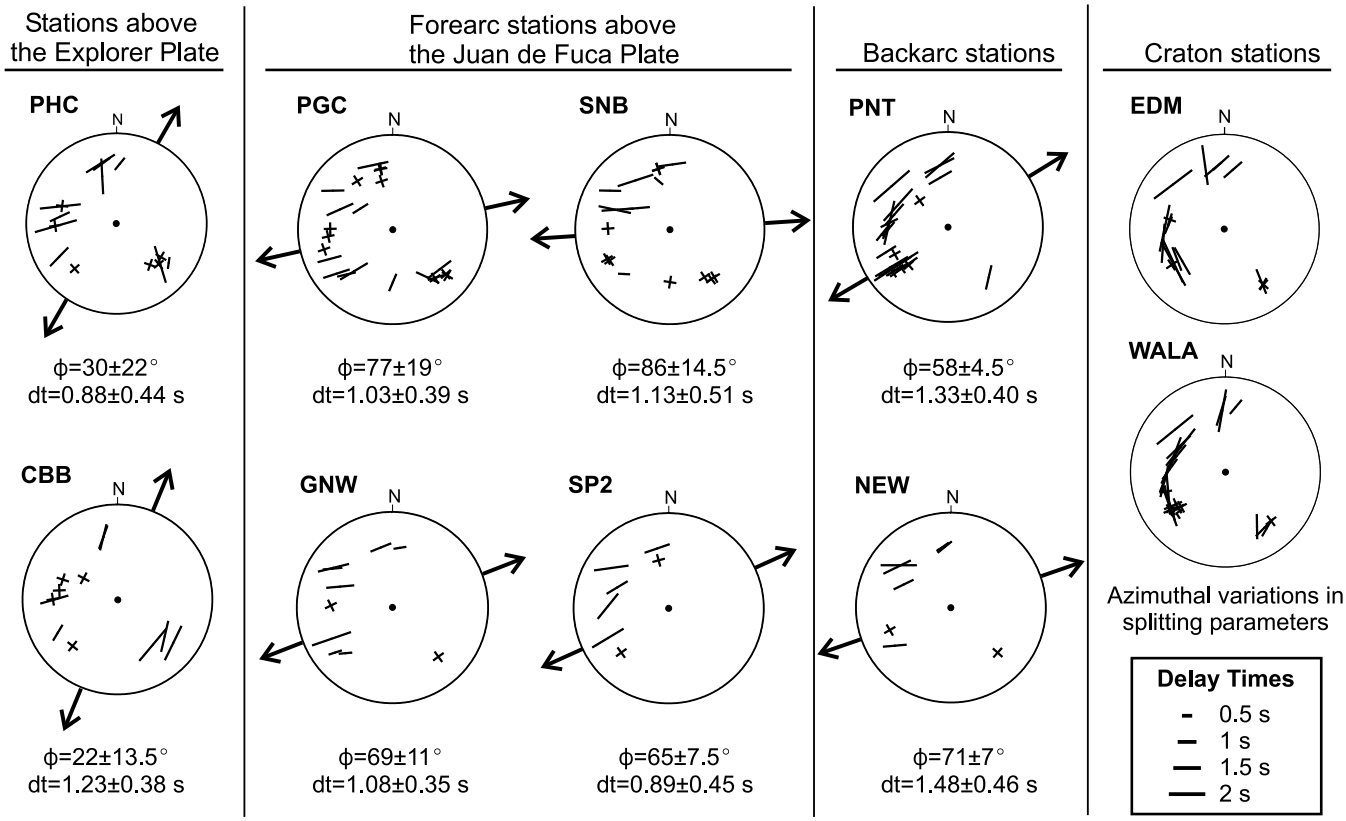

Figure 3. Lower hemisphere, equal-area projections of *SKS* splitting parameters at 10 stations. The outer circle corresponds to an incidence angle of 15°. The orientation of each bar indicates the fast direction; bar length is proportional to the delay time (see legend). A cross indicates a null measurement, with one arm of the cross parallel to the fast direction given by the splitting analysis. The arrows outside the circle show the fast direction obtained from stacking all non-null measurements at each station. Below each plot, the stacked values from the fast directions (ϕ) and delay times (dt) are shown, with 95 per cent confidence intervals. The splitting parameters at EDM and WALA show an azimuthal dependence, and thus an average fast direction was not calculated (see text).

earthquakes from a wide range of azimuths. One previous measurement at this station by Bostock & Cassidy (1995) yielded a north–south fast direction and a small delay time of 0.3 s.

3.2 Backarc observations

Shear wave splitting was observed at five of the seven stations that are located in the backarc of the Cascadia subduction zone. At station PIN, a single high-quality waveform yielded a fast direction of N64°E ± 1.5° and delay time of 2.1 ± 0.1 s. At stations HNB, HAWA, PNT and NEW the fast directions are oriented N58°E to N74°E, with delay times of 1.1 to 1.5 s. At station PNT, Bostock & Cassidy (1995) obtained a fast direction of 51°, fairly close to our value of 58 ± 4.5°. They observed a delay time of 1.70 s, slightly larger than our delay time of 1.33 ± 0.40 s.

At the two most northerly stations (LLLB and SLEB), no clear splitting could be identified for most earthquakes from a wide range of azimuths. At the now-closed station PMB, ∼85 km west of LLLB, Bostock & Cassidy (1995) observed *SKS* splitting with a NE–SW fast direction and a delay time of 0.65 s for three waveforms.

3.3 North America craton observations

The Rocky Mountain Trench marks the eastern edge of the Cascadia backarc (Hyndman & Lewis 1999). Two stations (EDM and WALA) are located east of this, on the North America craton. Clear splitting was observed at both stations. At each station, the fast directions show significant variations with earthquake azimuth (Fig. 3). Thus, we did not calculate a single set of splitting parameters. At station WALA, Bostock & Cassidy (1995) obtained an average fast direction oriented NE–SW and a delay time of 0.90 s for eight *SKS* waveforms, but they noted that there were azimuthal variations in the individual splitting parameters. At station EDM, three splitting measurements by Bostock & Cassidy (1995) give a fast direction of 33° and a delay time of 0.60 s. This delay time is much smaller than the majority of our observations.

4 DISCUSSION

The above observations show that significant seismic anisotropy occurs beneath the active Cascadia subduction zone and the adjacent stable North America craton. Seismic anisotropy measurements made using *SKS* phases represent the integrated effect of anisotropy in a vertical column beneath each station. Although these measurements have a high degree of lateral resolution, it is difficult to resolve the thickness or degree of anisotropy below the station, making the depth resolution rather poor.

The majority of stations exhibit delay times greater than 1.0 s. Such delay times are too large for anisotropy to be confined to the continental crust. The crustal thickness is ∼35 km throughout the Cascadia forearc and backarc regions (Clowes *et al.* 1995; Burianyk *et al.* 1997). Within the western North America craton, the crust is ∼50 km thick (Burianyk *et al.* 1997). If a delay time of 1.0 s were produced by only anisotropy within the crust, anisotropy of 7–10 per cent would be required, assuming an average crustal shear wave

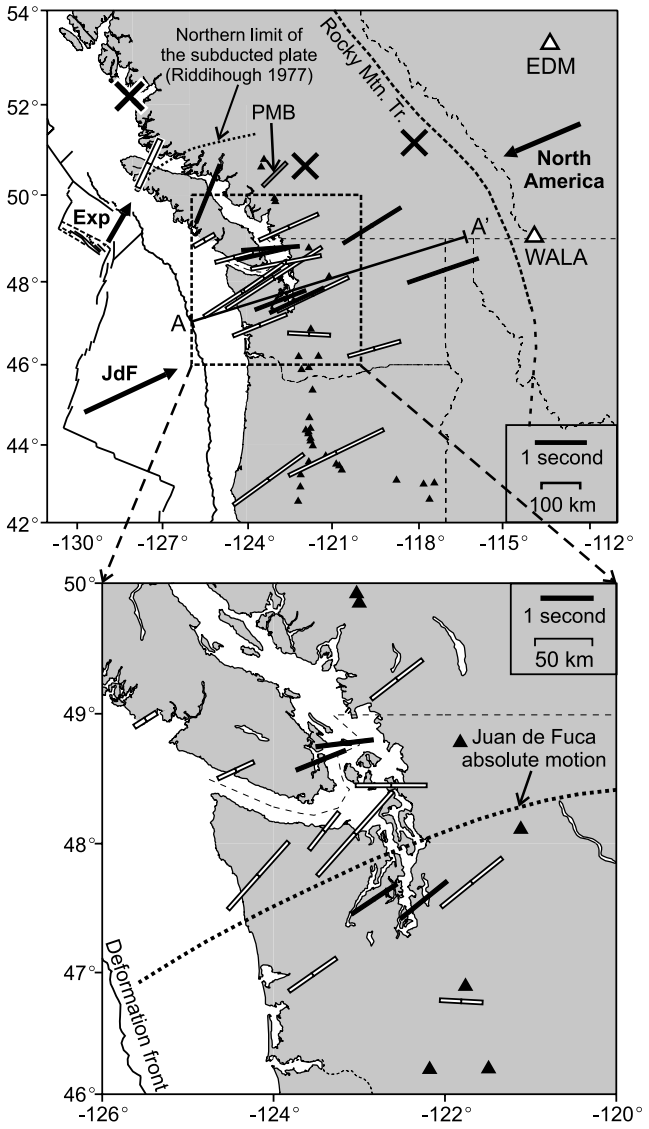

Figure 4. Stacked shear wave splitting parameters at each station. Orientation of bar indicates fast direction; bar length is proportional to delay time. Solid bars indicate well-constrained results; open bars indicate more poorly constrained results (see text). Results for PMB are from Bostock & Cassidy (1995). An azimuthal dependence of the splitting parameters was observed at stations WALA and EDM (see text). Arrows in the upper figure indicate the absolute plate motion of the Explorer (Ristau *et al.* 2002), Juan de Fuca and North America plates (Gripp & Gordon 2002). The dotted line in the lower figure shows the variations in the direction of absolute plate motion of the Juan de Fuca plate. Line A–A′ (upper figure) shows the profile used in Fig. 5. Solid triangles are active volcanoes.

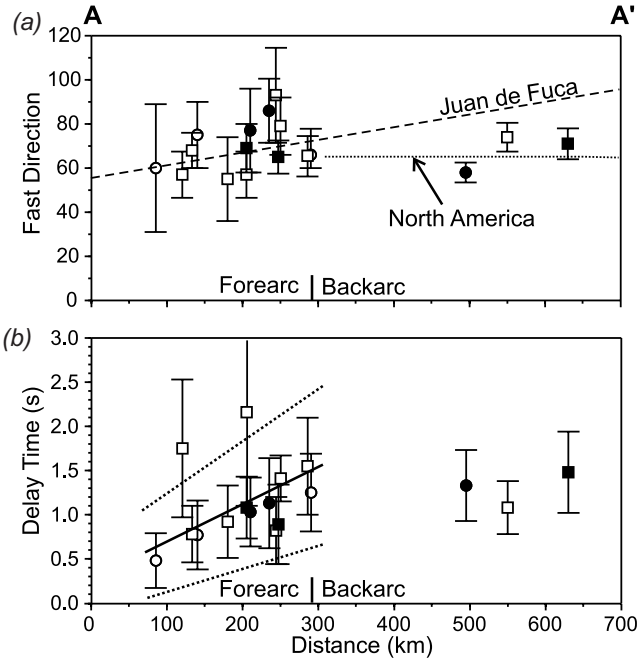

Figure 5. Projection of splitting parameters onto a margin-normal profile line (see Fig. 4 for location). Circles are Canadian stations; squares are US stations. Solid symbols indicate well-constrained results; open symbols indicate fair results. Error bars indicate the 95 per cent confidence interval for each value. (a) Fast directions. Absolute plate motion direction for the Juan de Fuca and North America (minus 180°) plates are given (Gripp & Gordon 2002). (b) Delay times. The weighted best fit line (with 1σ uncertainties) for the increase in forearc delay times is shown.

velocity of 3.6 km s^{-1}. This is much larger than typical values for crustal material (Silver & Chan 1991; Savage 1999 and references therein). In addition, observations of crustal anisotropy within the Cascadia forearc constrain anisotropy in the crust to be 2 per cent or less (Cassidy & Bostock 1996; Currie *et al.* 2001). Thus, we attribute the majority of the observed *SKS* splitting to anisotropy within the mantle and subducting crust beneath each station.

4.1 Anisotropy beneath the Juan de Fuca forearc

At forearc stations above the Juan de Fuca Plate, the fast directions are oriented approximately N70°E, with delay times at most stations greater than 1.0 s. The *SKS* phase observed at each station must pass through the crust, subducting Juan de Fuca Plate and underlying mantle, and, in some cases, the forearc mantle wedge above the subducting plate.

As noted above, the large delay times require that the most of the *SKS* anisotropy originate below the overriding continental crust. Fig. 5 shows a projection of the splitting parameters for the Washington and southern British Columbia stations onto a profile line oriented normal to the trench (see Fig. 4 for profile location). The observed fast directions are approximately parallel to the direction of absolute motion of the Juan de Fuca Plate (Gripp & Gordon 2002). The agreement between the observed fast directions and absolute plate motions suggests that the observed *SKS* anisotropy may be primarily due to lattice-preferred orientation (LPO) in the mantle beneath the Juan de Fuca Plate, resulting from mantle deformation associated with plate motion.

This anisotropy may result either from fossil anisotropy in the cool (<900 °C) part of the subducting lithosphere or from actively produced anisotropy from present-day mantle deformation below the subducting plate. The Juan de Fuca Plate is very warm due to its young age (6 to 8 Myr) and ∼3 km thick insulating sediment cover. Thermal modelling shows that temperatures of 900 °C are reached ∼20 km below the top of the plate (Hyndman & Wang 1993). To produce a delay time of 1.0 s, fossil anisotropy of at least 8 per cent would be required in this 20 km thick layer. In one study, Hiramatsu *et al.* (1997) suggest a maximum anisotropy of 5 per cent within the subducting plate beneath Japan. Matcham *et al.* (2000) observed anisotropy of 4.4 ± 0.9 per cent for the subducting plate at the southern end of the Hikurangi subduction zone. Thus, although the cool subducting lithosphere may be anisotropic, the observed

delay times require additional anisotropy in the warm (>900 °C) mantle beneath the plate.

Anisotropy of 4 to 5 per cent has been observed in mantle xenoliths from southern British Columbia (Saruwatari *et al.* 2001), as well as other regions (Mainprice & Silver 1993; Ji *et al.* 1994). Assuming a mean shear wave velocity of 4.5 km s^{-1}, it would be necessary to have a ∼100 km thick mantle layer with 5 per cent anisotropy to produce 1.0 s of splitting. At the Hikurangi subduction zone, observations suggest that anisotropy below the subducting lithosphere may be less than 1.4 per cent (Gledhill & Stuart 1996; Matcham *et al.* 2000). If anisotropy beneath the Juan de Fuca Plate decreases with depth, the thickness of the layer below the subducting plate would have to be much greater (up to 250 km thick) to produce the observed delay time. If subduction-related, the anisotropic layer is expected to dip at the same angle as the subducting plate. The dip of the Juan de Fuca Plate is quite shallow beneath much of the Cascadia forearc, increasing from 10–15° beneath the Pacific coast to 20–25° beneath Puget Sound and southeastern Vancouver Island (Flück *et al.* 1997). Modelling of the shear wave splitting parameters for a dipping anisotropic layer shows that both the fast directions and delay times will exhibit azimuthal variations (e.g. Savage 1999; Hartog & Schwartz 2000). However, for a dip of less than 30°, the azimuthal variations are within the uncertainties of the splitting parameters.

Effect of forearc crustal anisotropy

The observed *SKS* anisotropy is consistent with a model of mantle deformation associated with subduction. Studies of crustal anisotropy in this region using shear waves from local earthquakes have clearly shown that the overriding crust is also anisotropic (Cassidy & Bostock 1996; Currie *et al.* 2001). The fast directions within the crust are oriented parallel to the strike of the subduction zone, approximately perpendicular to the fast directions observed for the *SKS* waveforms. The delay times show a small increase with focal depth (to a maximum of 0.35 s for earthquakes at 35–40 km depth), suggesting an average of 1–2 per cent anisotropy for the forearc lithosphere, with the majority of the anisotropy within the upper 10–20 km.

Although the thin layer of crustal anisotropy will affect the *SKS* waveform (Rumpker & Silver 1998; Saltzer *et al.* 2000), the effects are probably small. No significant azimuthal variations were observed in the *SKS* splitting parameters that would be indicative of multiple layers of anisotropy. The fast direction within the crust is nearly perpendicular to the observed *SKS* fast direction. For two layers with perpendicular fast directions, little azimuthal variation in the splitting parameters would be expected. The main effect of the crustal layer would be to produce a reduced delay time at the surface. From the local shear wave splitting studies, the maximum crustal delay times were ∼0.35 s (Cassidy & Bostock 1996; Currie *et al.* 2001). Thus, the actual delay times due to mantle anisotropy alone may be 0.35 s longer than observed in the *SKS* waveforms. The crustal measurements were made using high-frequency shear waves from local earthquakes, with periods of 0.1 to 1 s. For the long-period (>8 s) *SKS* waves, the effective crustal anisotropy is probably smaller due to the much longer wavelength of the *SKS* energy relative to the inferred 10–20 km thickness of the crustal anisotropy. A detailed study of crustal anisotropy within the Juan de Fuca forearc at longer periods is required to provide stronger constraints on the effect of the crustal layers on the *SKS* waveform.

Margin-perpendicular trends in delay times

A projection of the *SKS* delay times for the Juan de Fuca forearc stations onto the margin-normal profile shows that there is a systematic increase in delay times, from 0.7 s at coastal stations to over 1.5 s at stations 300 km inland (Fig. 5b). The weighted best-fit line has a slope of 0.0038 ± 0.0018 s km^{-1}. This increase may be due to a landward increase in the degree of mantle anisotropy below the subducting plate. Alternatively, anisotropy in the forearc mantle wedge above the subducting plate may explain this observation. The thickness of the continental crust in this region is ∼36 km (Clowes *et al.* 1995). The Juan de Fuca Plate is at a depth of ∼40 km beneath stations PGC and GNW, and at a depth of 70 km beneath the most easterly forearc stations (e.g. TTW, LON) (Flück *et al.* 1997), leading to an increase in mantle wedge thickness of ∼30 km across the forearc. To explain the observed increase in delay times, anisotropy of 3 to 5 per cent within this triangular wedge is required. This is well within estimates of mantle anisotropy. The fast direction of anisotropy would have to be in the direction of subduction, parallel to the inferred fast direction beneath the subducting plate (Fig. 6).

Seismic evidence suggests that the forearc mantle wedge is up to 60 per cent serpentinized (Bostock *et al.* 2002; Brocher *et al.* 2003; Hyndman & Peacock 2003). Laboratory experiments on serpentinized peridotite show that even a small amount of serpentine will dramatically reduce the strength of the rock, such that deformation is accommodated primarily by serpentine; the olivine is relatively undeformed (Escartin *et al.* 2001). In this case, LPO of olivine will not be developed by present-day deformation of the forearc mantle wedge. However, mantle wedge anisotropy may represent relict anisotropy from earlier deformation, or may result from the alignment of vertical fluid-filled cracks or heterogeneities in the distribution of serpentine within the wedge. In addition, serpentine is a highly anisotropic mineral (Kern *et al.* 1997), such that a grain-scale preferred orientation of serpentine could produce large-scale

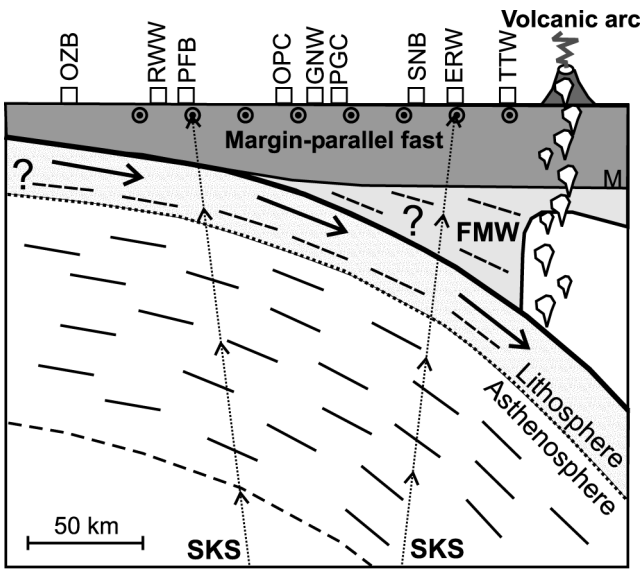

Figure 6. Model for forearc anisotropy. *SKS* observations require a ∼100 km thick anisotropic (4 to 5 per cent) layer in the mantle beneath the subducting plate, with a fast direction parallel to Juan de Fuca absolute plate motion (solid lines). The upper 10 to 20 km of the overriding continental crust are anisotropic with a margin-parallel fast direction, due to along-margin compressive stress. The forearc mantle wedge (FMW) may also be anisotropic (3 to 5 per cent) with a fast direction parallel to plate motion (dashed lines). M = continental Moho.

wedge anisotropy. It is not possible to distinguish between these mechanisms using only *SKS* splitting observations.

Some support for an anisotropic forearc mantle wedge is provided by *Pn* anisotropy observations that show a NE–SW fast direction in the forearc beneath Puget Sound, with up to 6 per cent *P*-wave anisotropy (Hearn 1996). No evidence for an anisotropic mantle wedge was observed for shear waves from Juan de Fuca Plate earthquakes (depths of 80–95 km) that travelled through the mantle wedge (Currie *et al.* 2001). However, the predicted delay time (∼0.4 s) through the wedge is similar to that observed for the overlying crust and to the period of the local shear waves. Thus, anisotropy within the upper crustal layer will dominate the observed shear wave splitting of this energy (Rumpker & Silver 1998). In order to resolve anisotropy in the forearc mantle wedge, it would be necessary to look at the frequency dependence of shear wave splitting parameters using locally generated shear waves. Such an analysis would also be useful for constraining the effects of the crustal anisotropic layer on longer-period seismic energy.

4.2 Along-margin variations in forearc shear wave splitting

The *SKS* splitting observations at stations located within the forearc above the Juan de Fuca Plate show fast directions that are parallel to the subduction direction, suggesting that the anisotropy may be primarily due to mantle deformation associated with subduction. Similar fast directions were observed in previous studies that looked at the southern end of the Cascadia subduction zone (Ozalaybey & Savage 1995; Hartog & Schwartz 2000; Schutt & Humphreys 2001 and references therein). This suggests a very uniform pattern of mantle deformation from central Vancouver Island to northern California.

For stations CBB and PHC, inland of the Explorer Plate, the observed fast directions are oriented approximately 45° more northerly than those observed in the forearc above the Juan de Fuca Plate (Fig. 4). The delay times at PHC and CBB suggest a mantle source for the anisotropy, most probably deformation-induced LPO of anisotropic mantle minerals. Seafloor magnetic anomaly analysis, GPS observations and earthquake focal mechanism studies indicate that Explorer Plate convergence is more northerly than that of the Juan de Fuca Plate (Riddihough 1977; Mazzotti *et al.* 2002; Ristau *et al.* 2002). This region also represents a transition zone from subduction of the Juan de Fuca Plate to margin-parallel transcurrent motion along the Queen Charlotte Fault. The northern limit of the subducted plate beneath northern Vancouver Island is inferred to be approximately 50 km southwest of station PHC (Riddihough 1977). Receiver function studies confirm that there is no evidence for a subducting plate beneath station PHC (Cassidy *et al.* 1998). Thus, the ∼N25°E fast directions observed at CBB and PHC may reflect the combination of the more northerly direction of mantle deformation due to Explorer plate subduction, as well as a change in mantle deformation related to the transition from subduction to along-margin strike-slip motion.

At station BBB, north of the triple junction, no clear anisotropy could be identified in our study, suggesting that there is no strong homogeneous horizontal flow pattern in the mantle beneath this region to develop anisotropy through LPO. This station is located almost 300 km east of the Queen Charlotte Fault. Mantle deformation associated with motion along the fault would be expected to be parallel to the fault. The numerous null measurements of this study and the small delay time reported by Bostock & Cassidy (1995) may indicate that mantle strain is confined to a relatively narrow region near the fault. Alternatively, highly complex mantle flow associated with this transitional region would also produce near-null splitting results.

4.3 Backarc anisotropy

For the backarc stations with clear splitting, the observed fast directions are intermediate between the absolute plate motion directions of the Juan de Fuca and North America plates (Fig. 5a). Surface heat flow measurements across the backarc show high values of 80 to 100 mW m^{-2} (Hyndman & Lewis 1999 and references therein). Thermal models of the backarc region indicate that the base of the crust is at a temperature of 800–1000 °C (Hyndman & Lewis 1999). High temperatures at shallow depths are confirmed by xenolith studies (Ross 1983; Saruwatari *et al.* 2001). In addition, *Pn* velocities in this region are low (∼7.8 km s^{-1}), suggesting temperatures in excess of 800 °C at the Moho (Hyndman & Lewis 1999). High temperatures (>900 °C) within the shallow backarc mantle imply that present-day ongoing mantle deformation is likely the cause of the observed shear wave anisotropy.

Xenoliths from depths of 45 km near station PNT show a strong lattice-preferred orientation of olivine (Saruwatari *et al.* 2001), confirming deformation of the uppermost mantle. The average shear wave anisotropy measured in these samples is 4.8 per cent, although the orientation of the anisotropy is not constrained. Assuming that the maximum anisotropy is in the horizontal plane and a mean shear wave velocity of 4.5 km s^{-1}, a layer thickness of ∼120 km is required to produce the observed average delay time of 1.3 s. For the maximum anisotropy in other orientations, the effective anisotropy for vertically propagating *SKS* waves would be less than that observed in the xenolith samples, and a slightly thicker anisotropic layer would be required.

Mantle anisotropy is only produced by dislocation creep of anisotropic mantle minerals (Karato 1987; Nicolas & Christensen 1987; Karato 1989). The maximum depth of anisotropy is proposed to be related to the pressure- and temperature-dependent rheological transition from dislocation creep to diffusion creep (Karato 1992). The presence of water will enhance this transition. As previously noted, the Cascadia backarc is an extremely hot, tectonically active area. In addition, the mantle wedge above the plate is probably hydrated, due to fluid released by dehydration of the subducting slab. For such a hot and wet region, the depth of the dislocation–diffusion creep transition is predicted to occur at depths of less than 250 km (Karato 1992).

These arguments suggest that anisotropy below the Cascadia backarc may be limited to fairly shallow depths in the mantle. The depth of the subducting Juan de Fuca Plate increases from 80 km beneath the volcanic arc to ∼300 km beneath PNT (Bostock & Van Decar 1994). Although anisotropy within the subducting plate or in the mantle beneath the plate cannot be ruled out by the observations, anisotropy within the mantle wedge may be sufficient to explain the observed *SKS* splitting.

The observed fast directions are consistent with subduction-induced mantle wedge corner flow, where a flow cell is generated in the wedge by the entrainment of the lowermost mantle wedge material by the subducting plate. High strain rates associated with this flow may produce LPO of anisotropic mantle minerals, leading to an overall anisotropic structure for the mantle wedge, with a fast direction parallel to the direction of convergence (Ribe 1989). The two northernmost backarc stations (LLLB and SLEB) are just south of the projected northern edge of the subducted plate (Riddihough 1977). The absence of significant shear wave splitting

at these stations may reflect a region of the mantle that is undergoing complex deformation, perhaps associated with flow around the northern edge of the subducted plate.

While both *SKS* splitting observations and mantle xenoliths indicate that the upper mantle in the Cascadia backarc is anisotropic, seismic refraction studies in the southern Canadian Cordillera have found little evidence for strong (>2 per cent) *Pn* anisotropy at regional scales (Clowes *et al.* 1995). Saruwatari *et al.* (2001) suggest that lithological or structural heterogeneities may be the reason for the absence of *Pn* anisotropy. The high lateral resolution of vertically propagating *SKS* waves means that the effects of lateral crustal heterogeneities are small. In eastern Washington State, Zervas & Crosson (1986) observed *Pn* velocity anisotropy of ∼2 per cent with a fast direction NW–SE. This direction is almost perpendicular to the fast directions inferred from *SKS* shear wave splitting. Hearn (1996) found ∼3 per cent *Pn* anisotropy with an east–west fast direction for most of Washington State east of the volcanic arc, in better agreement with our results. Only the southeast corner of Washington showed a fast direction oriented NW–SE, similar to the observations of Zervas & Crosson (1986).

Anisotropy has been observed in backarcs of subduction zones worldwide. Surprisingly, few regions exhibit fast directions parallel to the convergence direction. In many cases, the fast directions are highly oblique to the direction of convergence (Savage 1999 and references therein), indicating that the model of 2-D subduction-driven mantle wedge flow may not be adequate to explain shear wave anisotropy for all regions. It has been well documented that the backarcs of subduction zones in New Zealand, Japan, Kuril and Alaska have fast directions parallel to the strike of the subducting plate (e.g. Ando *et al.* 1983; Fouch & Fischer 1996; Gledhill & Gubbins 1996; Yang *et al.* 1995). Many subduction zones with trench-parallel fast directions are characterized by trench-parallel deformation of the upper plate. Fischer *et al.* (1998) suggest that backarc mantle strain may be primarily the result of recent motion of the overriding plate, as opposed to mantle flow driven by the subducting plate. Our observations are consistent with this alternative model for backarc mantle deformation. For the Cascadia backarc, there is currently no significant along-margin deformation of the upper plate. There are numerous margin-parallel strike-slip faults within the backarc crust, but geological evidence suggests that the last motion along these faults was in the early Cenozoic (Gabrielse 1991). The most recent episode of deformation was in the Eocene when the eastern part of the Cordillera underwent east–west extension (Gabrielse 1991). Since that time, the backarc crust has been moving to the southwest with the North American craton. Both the Eocene extension event, as well as ongoing southwestward motion, could produce LPO of the uppermost backarc mantle, with a fast direction oriented in the direction of convergence.

4.4 Multiple layers of anisotropy below the western North America craton?

The two craton stations (WALA and EDM) exhibit significant azimuthal variations in the shear wave splitting parameters. Azimuthal variations have been observed in other anisotropy studies near the western edge of the North American craton. Savage *et al.* (1996) reported azimuthal variations in the splitting parameters for teleseismic *S* waves at stations distributed across the Rocky Mountain Front south of 41°N, but did not have enough data to determine the cause of the variations. Schutt & Humphreys (2001) also observed complex anisotropy at stations near the Yellowstone Swell, which they attributed to multiple anisotropic layers or 3-D subsurface heterogeneities.

The azimuthal variations in the splitting parameters at WALA and EDM appear to have a 90° periodicity (Figs 7b and e), which is characteristic of layered anisotropy (Silver & Savage 1994). Although both dipping anisotropy and lateral variations in anisotropy produce azimuthal variations in splitting parameters, the variations do not have a 90° periodicity. In addition, to produce the observed large variations in the fast directions, it would be necessary to have a very steeply dipping layer of anisotropy. In this case, significant azimuthal variations in the delay times would be expected. Such variations are not observed at either station, although the delay time observations have large uncertainties. Although dipping anisotropy or lateral variations may be present in this region, we focus on layered anisotropy to explain the observations.

We have modelled the observed variations in the fast directions in terms of two layers of anisotropy, following Silver & Savage (1994). We primarily used the observations at WALA to constrain the model, due to the good azimuthal distribution of data at this station. In the model, we qualitatively fit the sharp jump in the observed fast directions between 50 and 60° backazimuth (modulo 90°) and the increase in fast direction with backazimuth (Fig. 7b). The two-layer model that best fits the fast direction observations has an upper layer with a fast direction N12°E and delay time of 1.4 s, and a lower layer with a fast direction of N81°E and delay time of 2.0 s (Fig. 7b). The estimated uncertainties in the fast direction and delay time for each layer are 15° and 0.3 s respectively. The parameters are not completely independent of one another. In particular, the position of the jump in the fast directions is highly sensitive to the ratio of the delay time in the lower layer to that of the upper layer. We find that a good fit is obtained if this ratio is 1.45 ± 0.2. The large delay times in each layer are required in order to fit the observed values of more than 1.0 s. Because the fast directions of the two layers are nearly perpendicular to each other, the observed delay time at the surface will be much less than that for the individual layers.

The rms difference between the modelled and observed fast directions at WALA is 11.9°. The observed fast directions fit this two-layer model much better than a single layer model. If the observations are stacked, the average fast direction is N24.6°E±20.0°. The rms difference between this single-layer model and the observations is 19.4°. The same two-layer model fits the observed fast directions at station EDM fairly well (Fig. 7e), with an rms difference of 17.2°. This fit is much better than a single-layer model using the observations at this station, where the rms difference is 31.1°. For both stations, the observed delay times are reasonably consistent with the proposed two-layer model (Figs 7c and f). The rms differences are 1.2 s and 1.5 s, at WALA and EDM respectively. At both stations, there are several observations near 55° backazimuth with fairly small delay times, whereas the model predicts maximum splitting values. In other regions, where two layers of anisotropy have been inferred, the observed delay times exhibit a large scatter in the region where the model predicts a peak in the delay times, and to date no observations have successfully matched the large theoretical peak (Ozalaybey & Savage 1995; Liu *et al.* 1995; Hartog & Schwartz 2001). Away from the predicted delay time peak, the observed delay times at WALA and EDM fit the two-layer model fairly well.

Due to the exact trade-off between anisotropic layer thickness and percentage anisotropy within the layer, it is not possible to constrain the thickness of each of the proposed layers from the modelled delay times alone. However, structural arguments allow us to place some constraints on the layer thickness. Station WALA is located

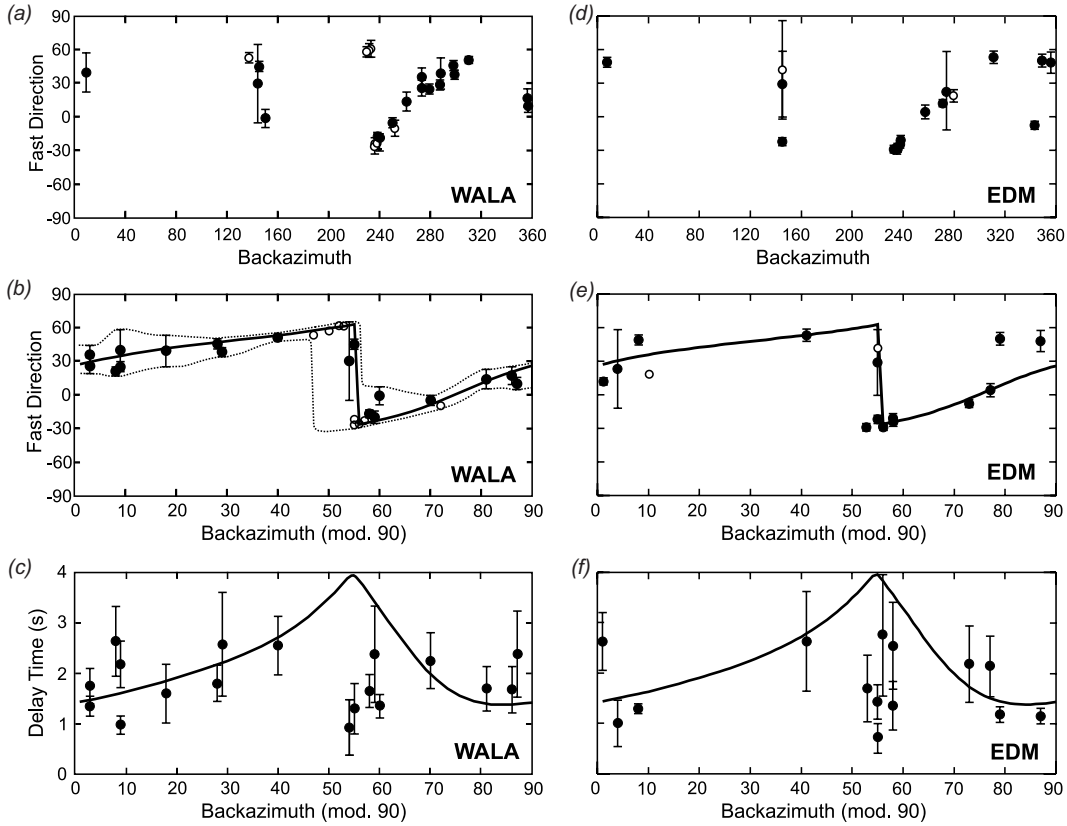

Figure 7. Observed fast directions (with 95 per cent confidence intervals) as a function of backazimuth at (a) WALA and (d) EDM. Open circles indicate null measurements. (b), (e) Fast directions and (c), (f) delay times as a function of backazimuth (modulo 90°) for each station. The solid line indicates the theoretical fast directions and delay times for a model containing two anisotropic layers. The upper layer has a fast direction of N12°E and delay time of 1.4 s. The lower layer has a fast direction of N81°E and delay time of 2.0 s. Dotted line in (b) shows the range of observational uncertainty.

on the North American craton, approximately 60 km east of the inferred eastern limit of the hot Cascadia backarc (Hyndman & Lewis 1999). Station EDM is located even further onto the North America craton. The North America craton is characterized by a surface heat flow of ∼45 mW m^{-2} (Hyndman & Lewis 1999), and high seismic velocities to more than 250 km depth (e.g. Grand 1994; Fredericksen *et al.* 2001). These observations suggest that the North America craton lithosphere is much thicker and cooler than that below the backarc. Due to the cooler craton lithosphere, it is unlikely that the uppermost mantle is currently undergoing deformation. We suggest that the two layers of anisotropy may correspond to a layer of fossil anisotropy within the thick craton lithosphere overlying an anisotropic layer produced by present-day deformation (Fig. 8).

The upper anisotropic layer in the model has a fast direction of N12°E and delay time of 1.4 s. Structural features such as aligned lithological units, magma bodies and fluid-filled cracks can produce anisotropy, but all are local features primarily found in the crust. If the proposed upper layer of anisotropy were uniformly distributed within the 50 km thick crust, an unreasonably large anisotropy of over 10 per cent would be needed to produce a delay time of 1.4 s. Structural anisotropy is likely concentrated in the uppermost crust, requiring even larger anisotropy. Thus, the proposed upper layer of anisotropy beneath WALA must extend into the lithospheric mantle. Silver & Chan (1991) suggest that anisotropy in stable continental regions may result from LPO developed during vertically coherent deformation of the crust and underlying mantle during a large-scale thermotectonic episode that is subsequently frozen in as the lithosphere cools below a temperature of 900 °C. For an average lithosphere anisotropy of 4 to 5 per cent (e.g. Mainprice & Silver 1993), a layer of thickness 130 to 160 km is required to produce the inferred delay time of 1.4 s. Thermal models and kimberlite xenolith data for the craton suggest that a temperature of 900 °C is reached at depths of 110 to 140 km (Hyndman & Lewis 1999 and references therein), in good agreement with the estimated thickness of the upper anisotropic layer. Although this entire region has experienced tectonism associated with collision and accretion during the Mesozoic, the majority of deformation has occurred in the upper 5 to 10 km, within sedimentary units (Gabrielse 1991). Geological evidence suggests that the underlying crust and mantle of the western North American craton have remained largely undeformed for over 250 Myr. This area once marked the western edge of the unextended part of the North America plate, and thus, the anisotropy may have been produced during pre-Mesozoic plate-boundary deformation, which has been preserved in the cool lithosphere.

In the model, the lower anisotropic layer has a fast direction of N81°E and delay time of 2.0 s. This layer may result from LPO developed by present-day deformation of the mantle at depths greater than 150 km. Assuming 4 to 5 per cent anisotropy within this layer, a thickness of ∼200 km would produce the inferred delay time, suggesting that anisotropy extends to depths greater than 350 km. Although strong anisotropy is generally inferred to be confined to depths less than 250 km for tectonically active areas, there is some evidence that the base of the anisotropic layer extends to greater depths beneath stable cratons, due to the much cooler temperatures

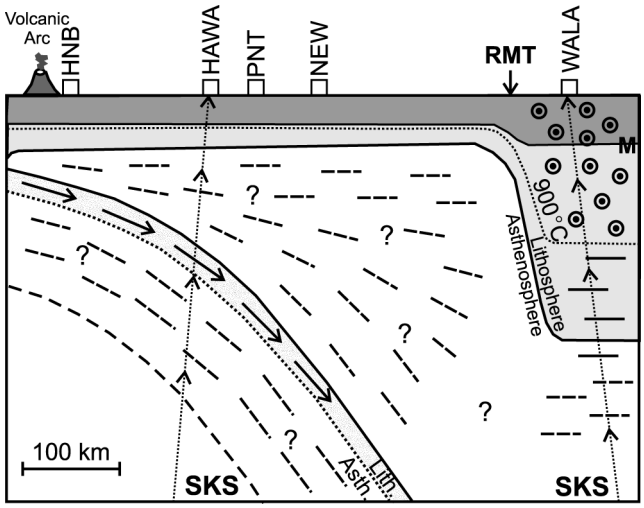

Figure 8. Tectonic model for shear wave anisotropy for the backarc and craton. The cross-section is oriented normal to the trench. The Rocky Mountain Trench (RMT) separates the thin (warm) backarc lithosphere from the thick (cool) craton lithosphere. Within the backarc, the anisotropy is attributed to present-day deformation of the mantle above the subducting plate, with the fast direction in the direction of convergence. Beneath the craton, a thickened lithosphere may result in two anisotropic layers: an upper layer of fossil anisotropy with a fast direction approximately perpendicular to the cross-section, and a lower layer produced by present-day anisotropy with a fast direction parallel to the cross-section. M = continental Moho.

in these regions (Karato 1992; Ji *et al.* 1994; Schutt & Humphreys 2001). The modelled fast direction for this layer is approximately east–west. Fast directions with a similar east–west orientation have been observed to the south in the Basin and Range region (Savage *et al.* 1990) and southern California (Polet & Kanamori 2002), as well as in the lower layer of a two-layer model in the vicinity of the San Andreas Fault (Silver & Savage 1994; Ozalaybey & Savage 1995; Hartog & Schwartz 2001; Polet & Kanamori 2002). Based on shear wave splitting observations, Silver & Holt (2002) have discussed the possibility of eastward flow of the deep mantle beneath western North America. The fast direction of the lower anisotropic layer in our model is consistent with this proposed large-scale eastward mantle flow.

Multiple layers of anisotropy may be a distinctive feature of the North American craton. Bokelmann & Silver (2000) suggest two layers of anisotropy beneath the North American craton to fit shear wave splitting observations and traveltime delays for *P* and *S* waves. Shear wave splitting observations over eastern North America can be explained to first order with a model of sublithospheric mantle flow, but small-scale lateral variations in the splitting parameters may require some contribution from a lithospheric anisotropic layer (Fouch *et al.* 2000). To fit shear wave splitting observations for the northeast US Appalachians, Levin *et al.* (1999) presented a two-layer model, which they suggest represents an upper layer of fossil anisotropy associated with past lithospheric deformation and a lower asthenospheric layer of anisotropy associated with present-day mantle flow. An additional complication comes from the possibility of a dipping anisotropic layer within the thick craton lithosphere. In a recent study, Bokelmann (2002) explained azimuthal variation in *P*-wave velocity at stations across the North American craton in terms of an anisotropic lithosphere with a fast axis dipping to the southwest. The data used by Bokelmann (2002) could not be used to resolve a lower layer of anisotropy. Teleseismic shear waves should record the presence of multiple layers of anisotropy, as well as dipping anisotropy within each layer (e.g. Levin *et al.* 1999). However, as the complexity of the anisotropic structure increases, it becomes difficult to infer the underlying anisotropic structure from shear wave splitting parameters alone. By combining traveltime observations with shear wave splitting measurements using high-quality data from a wide range of azimuths, further constraints may be placed on the anisotropic structure of the North American craton.

5 CONCLUSIONS

By analysing *SKS* waveforms recorded at 26 stations across the Cascadia subduction zone and western North American craton, we have constrained regional trends in shear wave anisotropy. For the majority of the Cascadia subduction zone forearc, the fast direction of shear wave anisotropy is parallel to absolute plate motion direction of the Juan de Fuca Plate. This may indicate subduction-related mantle deformation in a layer at least 100 km thick below the Juan de Fuca Plate. The delay times show an increase with distance from the deformation front. Although lateral variations in anisotropy below the subducting plate are not ruled out, anisotropy of 3 to 5 per cent in the forearc mantle above the plate may be sufficient to explain the observed increase in delay times. At the northern end of the Cascadia subduction zone, the fast directions rotate to a more northerly orientation, which may reflect a change in mantle deformation direction associated with the more northerly subduction direction of the Explorer Plate, as well as the transition from subduction to along-margin transform motion that occurs in this region.

Within the central backarc, the fast directions are parallel to the direction of convergence between the Juan de Fuca and North America plates. These observations support a model of mantle wedge anisotropy produced by subduction-induced mantle wedge corner flow. The two most northerly backarc stations show no clear shear wave splitting for data from a wide variety of azimuths, suggesting either that there is no strong horizontal anisotropy below these stations or that mantle anisotropy is highly complex. These stations may constrain the northern limit of the backarc mantle wedge flow cell. Although the backarc observations are compatible with the corner flow model, the observations can also be explained by deformation of the uppermost mantle associated with southwest motion of the overriding crust.

At two stations on the western North American craton, significant variations in the shear wave splitting parameters were observed, with a 90° periodicity. The observations were fitted with a two-layer model with an upper layer with an approximately north–south fast direction and a lower layer with a more east–west fast direction. The modelled delay times for each of the layers are 1.4 s and 2.0 s respectively, indicating thicknesses of ∼140 km and ∼200 km, for 4 to 5 per cent anisotropy. As the lithosphere of the North American craton is much thicker than that of tectonically active areas, the two layers may reflect an upper layer of fossil anisotropy underlain by an anisotropic layer produced by current mantle deformation.

ACKNOWLEDGMENTS

We thank Matt Fouch and Honn Kao for their careful reviews that improved the original manuscript. We acknowledge helpful discussions with David Eaton, Karen Fischer, Stephane Mazzotti and Bob Thompson. We thank Wendy McCausland and Steve Malone

(University of Washington) for providing some of the US data used in this study. Additional US data was obtained from the IRIS Data Management Center. Support for CC was provided by an NSERC graduate scholarship. Geological Survey of Canada contribution number 2003145.

REFERENCES

Ando, M., Ishikawa, Y. & Yamazaki, F., 1983. Shear wave polarization anisotropy in the upper mantle beneath Honshu, Japan, *J. geophys. Res.,* **88**, 5850–5864.

Bokelmann, G.H.R., 2002. Convection-driven motion of the North American craton: evidence from P-wave anisotropy, *Geophys. J. Int.,* **148,** 278–287.

Bokelmann, G.H.R. & Silver, P.G., 2000. Mantle variations within the Canadian Shield: traveltimes from the portable broadband Archean-Proterozoic Transect 1989, *J. geophys. Res.,* **105,** 579–605.

Bostock, M.G. & Cassidy, J.F., 1995. Variations in SKS splitting across western Canada, *Geophys. Res. Lett.,* **22,** 5–8.

Bostock, M.G. & Van Decar, J.C., 1994. Upper mantle structure of the northern Cascadia subduction zone, *Can. J. Earth Sci.,* **32,** 1–12.

Bostock, M.G., Hyndman, R.D., Rondenay, S. & Peacock, S.M., 2002. An inverted continental Moho and serpentinization of the forearc mantle, *Nature,* **417,** 536–538.

Braunmiller, J. & Nabelek, J., 2002. Seismotectonics of the Explorer region, *J. geophys. Res.,* **107**, (B10), 2208, doi: 10.1029/2001JB000220.

Brocher, T.M., Parsons, T., Tréhu, A.M., Snelson, C.M. & Fisher, M.A., 2003. Seismic evidence for widespread serpentinized forearc upper mantle along the Cascadia margin, *Geology,* **31,** 267–270.

Burianyk, M.J.A., Kanaswewich, E.F. & Udey, N., 1997. Broadside wide-angle seismic studies and three-dimensional structure of the crust in the southeast Canadian Cordillera, *Can. J. Earth Sci.,* **34,** 1156–1166.

Cassidy, J.F. & Bostock, M.G., 1996. Shear-wave splitting above the subducting Juan de Fuca plate, *Geophys. Res. Lett.,* **23,** 941–944.

Cassidy, J.F., Ellis, R.M., Karavas, C. & Rogers, G.C., 1998. The northern limit of the subducted Juan de Fuca plate system, *J. geophys. Res.,* **103,** 26 949–26 961.

Clowes, R.M., Zelt, C.A., Amor, J.R. & Ellis, R.M., 1995. Lithospheric structure in the southern Canadian Cordillera from a network of seismic refraction lines, *Can. J. Earth Sci.,* **32,** 1485–1513.

Crampin, S., 1977. A review of the effects of anisotropic layering on the propagation of seismic waves, *Geophys. J. R.. astr. Soc.,* **49,** 9–27.

Currie, C.A., Cassidy, J.F. & Hyndman, R.D., 2001. A regional study of shear wave splitting above the Cascadia subduction zone: margin-parallel crustal stress, *Geophys. Res. Lett.,* **28,** 659–662.

Escartin, J., Hirth, G. & Evans, B., 2001. Strength of slightly serpentinized peridotites: implications for the tectonics of oceanic lithosphere, *Geology,* **29,** 1023–1026.

Fischer, K.M., Fouch, M.J., Wiens, D.A. & Boettcher, M.S., 1998. Anisotropy and flow in Pacific subduction zone back-arcs, *Pure appl. Geophys.,* **151,** 463–475.

Flück, P., Hyndman, R.D. & Wang, K., 1997. Three-dimensional dislocation model for great earthquakes of the Cascadia subduction zone, *J. geophys. Res.,* **102,** 20 539–20 550.

Fouch, M.J. & Fischer, K.M., 1996. Mantle anisotropy beneath northwest Pacific subduction zones, *J. geophys. Res.,* **101,** 15 987–16 002.

Fouch, M.J. Fischer, K.M., Parmentier, E.M., Wysession, M.E. & Clarke, T.J., 2000. Shear wave splitting, continental keels, and patterns of mantle flow, *J. geophys. Res.,* **105,** 6255–6275.

Fredericksen, A.W., Bostock, M.G. & Cassidy, J.F., 2001. S-wave velocity structure of the Canadian upper mantle, *Phys. Earth planet. Int.,* **124,** 175–191.

Gabrielse, H. (Comp.), 1991. Structural styles, in, *Geology of the Cordilleran Orogen in Canada,* **4,** pp. 571–675, eds Gabrielse, H. & Yorath, C.J., Geological Survey of Canada, Geology of Canada.

Gledhill, K. & Gubbins, D., 1996. SKS splitting and the seismic anisotropy of the mantle beneath the Hikurangi subduction zone, New Zealand, *Phys. Earth planet. Int.,* **95,** 227–236.

Gledhill, K. & Stuart, G., 1996. Seismic anisotropy in the forearc region of the Hikurangi subduction zone, New Zealand, *Phys. Earth planet. Int.,* **95,** 211–225.

Grand, S.P., 1994. Mantle shear structure beneath the Americas and surrounding oceans, *J. geophys. Res.,* **99,** 11 591–11 621.

Gripp, A.G. & Gordon, R.G., 2002. Young tracks of hotspots and current plate velocities, *Geophys. J. Int.,* **150,** 321–361.

Hartog, R. & Schwartz, S.Y., 2000. Subduction-induced strain in the upper mantle east of the Mendocino triple junction, California, *J. geophys. Res.,* **105,** 7909–7930.

Hartog, R. & Schwartz, S.Y., 2001. Depth-dependent mantle anisotropy below the San Andreas fault system: apparent splitting parameters and waveforms, *J. geophys. Res.,* **106,** 4155–4167.

Hearn, T.M., 1996. Anisotropic Pn tomography in the western United States, *J. geophys. Res.,* **101,** 8403–8414.

Hiramatsu, Y., Ando, M. & Ishikawa, Y., 1997. ScS wave splitting of deep earthquakes around Japan, *Geophys. J. Int.,* **128,** 409–424.

Hyndman, R.D. & Lewis, T.J., 1999. Geophysical consequences of the Cordillera-Craton thermal transition in southern Canada, *Tectonophysics,* **306,** 397–422.

Hyndman, R.D. & Peacock, S.M., 2003. Serpentinization of the forearc mantle, *Earth planet. Sci. Lett.,* **212,** 417–432.

Hyndman, R.D. & Wang, K., 1993. Thermal constraints on the zone of major thrust earthquake failure: the Cascadia subduction zone, *J. geophys. Res.,* **98,** 2039–2060.

Ji, S., Zhai, X. & Francis, D., 1994. Calibration of shear-wave splitting in the subcontinental upper mantle beneath active orogenic belts using ultramafic xenoliths from Canadian Cordillera and Alaska, *Tectonophysics,* **239,** 1–27.

Karato, S., 1987. Seismic anisotropy due to lattice preferred orientation of minerals: kinematic or dynamic?, in, *High Pressure Research in Mineral Physics, Geophys. Monogr. Ser.,* **39,** pp. 455–471, eds Manghnani, M.H. & Syono, Y., AGU, Washington, DC.

Karato, S., 1989. Seismic anisotropy: mechanisms and tectonic implications, in, *Rheology of Solids and of the Earth,* pp. 393–422. eds Karato, S. & Toriumi, M., Oxford University Press, Oxford.

Karato, S., 1992. On the Lehmann discontinuity, *Geophys. Res. Lett.,* **19,** 2255–2258.

Kern, H., Liu, B. & Popp, T., 1997. Relationship between anisotropy of P and S wave velocities and anisotropy of attenuation in serpentinite and amphibolite, *J. geophys. Res.,* **102,** 3051–3065.

Levin, V., Menke, W. & Park, J., 1999. Shear wave splitting in the Appalachians and the Urals: a case for multilayered anisotropy, *J. geophys. Res.,* **104,** 17 975–17 993.

Liu, H., Davis, P.M. & Gao, S., 1995. SKS splitting beneath southern California, *Geophys. Res. Lett.,* **22,** 767–770.

Mainprice, D. & Silver, P.G., 1993. Interpretation of SKS-waves using samples from the subcontinental lithosphere, *Phys. Earth planet. Int.,* **78,** 257–280.

Matcham, I., Savage, M.K. & Gledhill, K.R., 2000. Distribution of seismic anisotropy in the subduction zone beneath the Wellington region, New Zealand, *Geophys. J. Int.,* **140,** 1–10.

Mazzotti, S., Flueck, P., Hyndman, R.D., Dragert, H., Craymer, M. & Schmidt, M., 2002. Tectonics of western Canada from GPS observations, *EOS, Trans. Am. geophys, Un.,* **83**(47), Fall Meet. Suppl., Abstract T71B–1176.

Nicolas, A. & Christensen, N.I., 1987. Formation of anisotropy in upper mantle peridotites: a review, in, *Composition, Structure and Dynamics of the Lithosphere–Asthenosphere System, Geodyn. Ser.,* **16,** pp. 111–123, eds Fuchs, K. & Froidevaux, C., AGU,Washington, DC.

Nuttli, O., 1961. The effect of the Earth's surface on the S wave particle motion, *Bull. seism. Soc. Am.,* **51,** 237–246.

Ozalaybey, S. & Savage, M.K., 1995. Shear-wave splitting beneath western United States in relation to plate tectonics, *J. geophys. Res.,* **100,** 18 135–18 149.

Polet, J. & Kanamori, H., 2002. Anisotropy beneath California: shear wave splitting measurements using a dense broadband array, *Geophys. J. Int.,* **149,** 313–327.

Ribe, N.M., 1989. Seismic anisotropy and mantle flow, *J. geophys. Res.,* **94,** 4213–4223.

Riddihough, R., 1977. A model for recent plate interactions off Canada's west coast, *Can. J. Earth Sci.,* **14,** 384–396.

Riddihough, R., 1984. Recent movements of the Juan de Fuca plate system, *J. geophys. Res.,* **89,** 6980–6994.

Ristau, J., Rogers, G. & Cassidy, J., 2002. Relative plate motions and stress orientation in western Canada from regional moment-tensor analysis, *Seis. Res. Lett.,* **73,** 261.

Rohr, K.M.M. & Furlong, K.P., 1995. Ephemeral plate tectonics at the Queen Charlotte triple junction, *Geology,* **23,** 1035–1038.

Ross, J.V., 1983. The nature and rheology of the Cordilleran upper mantle of British Columbia: inferences from peridotite xenoliths, *Tectonophysics,* **100,** 321–357.

Rumpker, G. & P.G. Silver, 1998. Apparent shear-wave splitting parameters in the presence of vertically varying anisotropy, *Geophys. J. Int.,* **135,** 790–800.

Saltzer, R.L., Gaherty, J.B. & Jordan, T.H., 2000. How are vertical shear wave splitting measurements affected by variations in the orientation of azimuthal anisotropy and depth?, *Geophys. J. Int.,* **141,** 374–390.

Saruwatari, K., Ji, S., Long, C. & Salisbury, M.H., 2001. Seismic anisotropy of mantle xenoliths and constraints on upper mantle structure beneath the southern Canadian Cordillera, *Tectonophysics,* **339,** 403–426.

Savage, M.K., 1999. Seismic anisotropy and mantle deformation: what have we learned from shear wave splitting?, *Rev. Geophys.,* **37,** 65–106.

Savage, M.K., Silver, P.G. & Meyer, R.P., 1990. Observations of teleseismic shear-wave splitting in the Basin and Range from portable and permanent stations, *Geophys. Res. Lett.,* **17,** 21–24.

Savage, M.K., Sheehan, A.F. & Lerner-Lam, A., 1996. Shear wave splitting across the Rocky Mountain Front, *Geophys. Res. Lett.,* **23,** 2267–2270.

Schutt, D.L. & Humphreys, E.D., 2001. Evidence for a deep asthenosphere beneath North America from western United States SKS splits, *Geology,* **29,** 291–294.

Silver, P.G. & Chan, W.W., 1991. Shear wave splitting and subcontinental mantle deformation, *J. geophys. Res.,* **96,** 16 429–15 454.

Silver, P.G. & Holt, W.E., 2002. The mantle flow field beneath western North America, *Science,* **295,** 1054–1057.

Silver, P.G. & Savage, M.K., 1994. The interpretation of shear-wave splitting parameters in the presence of two anisotropic layers, *Geophys. J. Int.,* **119,** 949–963.

Vinnik, L.P., Makeyeva, L.I., Milev, A. & Usenko, A.Y., 1992. Global patterns of azimuthal anisotropy and deformations in the continental mantle, *Geophys. J. Int.,* **111,** 433–447.

Wolfe, C.J. & Silver, P.G., 1998. Seismic anisotropy of oceanic upper mantle: Shear wave splitting methodologies and observations, *J. geophys. Res.,* **103,** 749–771.

Yang, X., Fischer, K.M. & Abers, G.A., 1995. Seismic anisotropy beneath the Shumagin Islands segment of the Aleutian-Alaska subduction zone, *J. geophys. Res.,* **100,** 18 165–18 177.

Zervas, C.E. & Crosson, R.S., 1986. Pn observation and interpretation in Washington, *Bull. seism. Soc. Am.,* **76,** 521–546.

Zhang, S. & Karato, X., 1995. Lattice preferred orientation of olivine aggregates deformed in simple shear, *Nature,* **375,** 774–777.